Green Chemistry Letters and Reviews

ISSN: (Print) (Online) Journal homepage: https://www.tandfonline.com/loi/tgcl20

Synthesis of luminescent semiconductor nanoparticles in ionic liquids –the importance of the ionic liquid in the formation of quantum dots

Meike Leu, Paul Campbell & Anja-Verena Mudring

To cite this article: Meike Leu, Paul Campbell & Anja-Verena Mudring (2021) Synthesis of luminescent semiconductor nanoparticles in ionic liquids –the importance of the ionic liquid in the formation of quantum dots, Green Chemistry Letters and Reviews, 14:1, 128-136, DOI: 10.1080/17518253.2021.1875057

To link to this article: https://doi.org/10.1080/17518253.2021.1875057

Published online: 27 Jan 2021.

GREEN CHEMISTRY LETTERS AND REVIEWS
2021, VOL. 14, NO. 1, 128–136
https://doi.org/10.1080/17518253.2021.1875057

Synthesis of luminescent semiconductor nanoparticles in ionic liquids –the importance of the ionic liquid in the formation of quantum dots

Meike Leu[a], Paul Campbell[a] and Anja-Verena Mudring[a,b]

[a]Department of Chemistry and Biochemistry, Ruhr-Universität Bochum, Bochum, Germany; [b]Department of Materials and Environmental Chemistry, Stockholm University, Stockholm, Sweden

ABSTRACT

Zinc sulfide (ZnS) and cadmium sulfide (CdS) nanoparticles were synthesized in different ionic liquids (IL) with microwave irradiation. Particle characterization by means of powder X-ray diffraction (PXRD), scanning electron microscopy (SEM) and optical spectroscopy (UV-vis absorption and photoluminescence) showed a strong dependence of the particle size depending on the IL employed. Whilst all ILs yielded particles in the nanometer regime and showed in their optical properties quantum confinement, particularly small particles were obtained from choline-base ILs pointing to the strong influence of this IL cation in blocking the particle growth. Here, quantum dots of 1.5–3 nm size were yielded for both, ZnS and CdS.

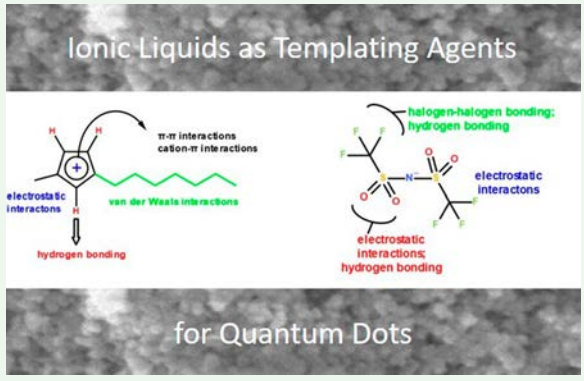

ARTICLE HISTORY
Received 10 September 2020
Accepted 7 January 2021

KEYWORDS
Cadmium sulfide; ionic liquids; microwave synthesis; quantum dots; zinc sulfide

Introduction

Ionic liquids (ILs) are frequently being discussed in the context of Green Chemistry (*1*). They are organic salts consisting of ions, with a melting point below 100°C (*2*). ILs often contain a bulky and asymmetric anions and cations which leads to a low melting point through (kinetic) inhibition of crystallisation (*3*). Other reasons for the low melting point are weak intermolecular interactions and a good charge distribution (*2*). They frequently feature a high polarity, low vapor pressure, high ionic conductivity, low toxicity, non-flammability, and thermal stability (*4*). These characteristics make them a good, often environmentally benign, alternative to organic solvents (*5*). Although the first ILs were already introduced in 1914, research on the use of ILs as solvents has only recently developed in the last few decades. Still, their application in inorganic materials synthesis is less explored compared to the attention they have been receiving in organic synthesis and catalysis. However, the extraordinary abilities of ILs bear strong advantages for the synthesis of nanoparticles (*6–9*). For example, many ILs exhibit a low interfacial tension, which leads to a high nucleation rate. Therefore small particles are obtained which experience only weak Ostwald ripening. Once formed, the particles can undergo Ostwald ripening only faintly as ILs form a protective electrostatic shell around nanoparticles (NPs) to prevent agglomeration (*10,11*). Through their interaction with the particle surface they can well work as templating agents, evoking special nanostructures, i.e. influencing the particle size, morphology as well as aggregation (*12–16*). For polymorphic materials, even control of the crystalline phase has been reported (*15,17*). A particular advantage of using ILs as synthesis

CONTACT Anja-Verena Mudring anja-verena.mudring@mmk.su.se

media over classical solvents is, that the addition of templating agents and surfactants can be omitted. The synthesis of Sb_2Te_3 nanomaterials for application as a thermoelectric material is a very illustrative example in this context (*18*,*19*).

Semiconductor nanoparticles have been a focus in recent research due to their extraordinary properties which differ to those of bulk solids. Once the radius of a semiconductor particle becomes smaller than that of the excitonic Bohr radius, quantum dots are formed. Through quantum confinement effects the band gap energy is widened, leading to a blue shift in the emission spectra. The threshold for quantum effects is given by the value of the Bohr radius of an exciton in the bulk material. With decreasing particle size, the band gap energy is increasing, and consequently a higher surface to volume ratio is obtained. This leads to radiative or nonradiative recombination of an exciton and influences strongly the optical properties of semiconductors such as zinc and cadmium sulfide (*20*,*21*).

Zinc sulfide is an intensively investigated semiconductor with a high refraction index and a high transmission with the visible range of light. It appears in two polymorphs, cubic zinc blende (sphalerite), the low temperature form, and wurtzite (hexagonal), the high temperature polymorph ZnS (*22*). The cubic form features a band gap of 3.54 eV for the bulk, whereas the hexagonal one has a higher band gap of 3.91 eV (*23*). The exitonic Bohr radius of ZnS semiconductor nanocrystals is 2.5 nm (*24*). All these characteristics make ZnS nanoparticles an interesting choice for many applications. They have been already used for a cathode ray tube, a crystal laser using streamer excitation, as a phosphor in thin film electroluminescent devices and as the main component in light-emitting diodes (LED) when they are doped (*25–30*).

Cadmium sulfide is also a widely investigated semiconductor nanomaterial like zinc sulfide. Like ZnS it is polymorphic: For CdS the cubic zinc blende form is the stable one at room temperature (*18*). However, several polymorphs, amongst them the wurtzite phase (hexagonal) as well as a number of polytypes, a NaCl type high pressure form as well as an orthorhombic polymorph have been reported (*22*,*31*,*32*). Wurtzite-type CdS features a band gap of 2.42 eV in the bulk (*33*), its excitionic Bohr radius is 5.8 nm (*34*). CdS semiconductor nanoparticles are especially interesting for optoelectronic solar energy conversion and photocatalysis due to its extraordinary photochemical activities and strong absorption and emission of visible light (*35–37*).

All these applications require a control of semiconductor size and size distribution due to their size dependent optical and electronic properties. Therefore, reliable and robust synthetic procedures that yield the desired quantum dots are needed. A number of different bottom-up and top-down synthetic methods have been explored for the synthesis of QDs (*38*,*39*).

ILs are high-suitable media for absorbing microwaves as they are constituted off large ions with high polarizability and conductivity (*40*,*41*). Upon irradiation with microwaves, extremely high heating rates are achieved which lead to a high formation rate of nuclei, which, in turn, which favors nanoparticle formation. Due to the short heating times, particle growth is not supported as with conventional heating which requires much longer heat treatment to achieve conversion. In addition, the ionic liquid acts as a NP-stabilizer, thus, no stabilizing agents are required, yet the ionic liquid can easily be removed from the particle surface, which finally declares the obvious advantage of ionic liquids. All this gives the combination of ionic liquids with microwave irradiation good prospects for the synthesis of inorganic QDs. In the past, we have already beneficially used ILs as solvents, and sometimes even as smart reaction partners, in the microwave synthesis of photocatalysts, luminescent nanophosphors and nanosized thermoelectric materials (*42–54*).

We observed frequently, that the IL had a crucial influence on the particle size, morphology as well as, in case of polymorphic materials, the crystalline phase that formed for metal chalcogenides and halide particles synthesized by microwave heating in ionic liquids (*42–52*). Different ILs yielded under otherwise similar reaction conditions, different products. A few studies on the preparation of ZnS (*55*) and CdS (*56*,*57*) particles by microwave reaction have appeared. However, a systematic study which allows to evaluate the influence of the IL on the product formation and is still lacking. This prompted us to develop and study the synthesis of ZnS and CdS semiconductor nanoparticles in different ILs under microwave irradiation.

Materials and methods

Instrumentation

Synthesis of the nanoparticles was carried out with single mode microwave operating at 2455 MHz (CEM Discover, Kamp-Lintfort, D). ^{1}H-NMR spectra of ionic liquids were collected on a DPX200 (Bruker, Germany) in d_6 dimethyl sulfoxide (DMSO-d_6). Powder-XRD measurements were carried out at a HUBER G670 diffractometer with molybdenum source (MoK_α irradiation, $\lambda = 709.23$ nm). The samples were situated in a class capillary with a diameter of 0.5 mm. The particle morphology was inspected by SEM (scanning electron microscopy; LEO 1530 Gemini). Gold was deposited on

the powder to obtain conductive samples. UV-Visible absorption spectra were measured at room temperature on solid powder samples using an Agilent Cary 5000 spectrometer using the internal diffuse reflection accessory. Fluorescence and phosphorescence measurements were performed on a Horiba JobinYvon Fluorolog-3 spectrometer with a continuous xenon lamp (450 W). Double gratings for the excitation and emission spectrometer are applied as monochromators. The signal is detected with a photomultiplier. For measurement, the powdered sample was filled into silica tubes and carefully positioned in the incoming beam in the sample chamber.

Synthesis and characterization

Butylmethylimidazolium tetrafluoroborate, [C_4mim][BF_4]. Butylmethylimidazolium chloride (14.52 g, 0.083 mol) was dissolved in acetone and sodium tetrafluoroborate (23.89 g, 0.083 mol) was added to the solution. The mixture was stirred for two days. Afterwards the salt was removed and the solvent was evaporated. The ionic liquid was dissolved in dichloromethane and the solvent was evaporated again. Then the product was dried in the vacuum.

^{1}H NMR (200 MHz, DMSO-d_6), δ/ppm: 0.8 (t, 3H, CH_2-CH_3), 1.2 (m, 2H, CH_2-CH_2-CH_3), 1.7 (m, 2H, CH_2-CH_2-CH_2), 3.8 (s, 3H, CH_3-N), 4. 1 (t, 2H, N-CH_2-CH_2), 7.6 (d, 2H, N-CH-CH-N), 8.9 (d, 1H, N-CH-N).

Butylmethylimidazolium bis(trifluoromethanesulfonyl)amide, [C_4mim][NTf_2]. Butylmethylimidazolium chloride (14.4 g, 0.083 mol) was dissolved in water and lithium bis (trifluoromethanesulfonyl)amide (23.76 g, 0.083 mol) was added to the solution. The mixture was stirred for four hours. Next the mixture was dissolved in dichloromethane and the water layer was separated. Then the dichloromethane layer was washed with water until all halogens were removed. This was tested with a silvernitrate solution. The solvent was evaporated and the ionic liquid dried in vacuum.

^{1}H NMR (200 MHz, DMSO-d_6), δ/ppm: 0.0.9 (t, 3H, CH_2-CH_3), 1.3 (m, 2H, CH_2-CH_2-CH_3), 1.8 (m, 2H, CH_2-CH_2-CH_2), 3.8 (s, 3H, CH_3-N), 4.1 (t, 2H, N-CH_2-CH_2), 7.6 (d, 2H, N-CH-CH-N), 8.9 (s, 1H, N-CH-N).

Butylmethylimidazolium dicyanamide, [C_4mim][DCA]. Butylmethylimidazolium chloride (12.26 g, 0.0702 mol) was dissolved in acetone and sodium dicyanamide (6.25 g, 0.0702 mol) was added to the solution. The mixture was stirred for two days. Afterwards the salt was removed and the solvent was evaporated. The ionic liquid was dissolved in dichloromethane and the solvent was evaporated again. Then the product was dried in the vacuum.

^{1}H NMR (298 K, 200 MHz, DMSO-d_6), δ/ppm 0.9 (t, 3H, CH_2-CH_3), 1.3 (m, 2H, CH_2-CH_2-CH_3), 1.8 (m, 2H, CH_2-CH_2-CH_2), 3.9 (s, 3H, CH_3-N), 4.2 (t, 2H, N-CH_2-CH_2), 7.7 (d, 2H, N-CH-CH-N), 9.1 (s, 1H, N-CH-N).

Butylmethylpyridinium tetrafluoroborate, [C_4mpyr][BF_4]. Butylmethylpyridinium bromide (20 g, 0.087 mol) was dissolved in acetone and sodium tetrafluoroborate (9.54 g, 0.087 mol) was added to the solution. The mixture was stirred for two days. Afterwards the salt was removed and the solvent was evaporated. The ionic liquid was dissolved in dichloromethane and the solvent was evaporated again. Then the product was dried in the vacuum.

^{1}H NMR (200 MHz, DMSO-d_6), δ/ppm: 0.9 (t, 3H, CH_2-CH_3), 1.3 (m, 2H, CH_2-CH_2-CH_3), 1.9 (m, 2H, CH_2-CH_2-CH_2), 2.6 (s, 3H, CH_3-pyr), 4.5 (t, 2H, N-CH_2), 7.9 (d, 2H, pyr), 8.9 (d, 2H, pyr).

Butylmethylpyridinium bis(trifluoromethanesulfonyl)amide, [C_4mpyr][NTf_2]. Butylmethylpyridinium bromide (20 g, 0.087 mol) was dissolved in water and lithium bis (trifluoromethanesulfonyl)amide (24.98 g, 0.087 mol) was added to the solution. The mixture was stirred for four hours. Next the mixture was dissolved in dichloromethane and the water layer was separated. Then the dichloromethane layer was washed with water until all halogens were removed. This was tested with a silvernitrate solution. The solvent was evaporated and the ionic liquid dried in the vacuum.

^{1}H NMR (200 MHz, DMSO-d_6), δ/ppm: 0.9 (t, 3H, CH_2-CH_3), 1.3 (m, 2H, CH_2-CH_2-CH_3), 1.9 (m, 2H, CH_2-CH_2-CH_2), 2.9 (s, 3H, CH_3-pyr), 4.5 (t, 2H, N-CH_2), 7.9 (d, 2H, pyr), 8.9 (d, 2H, pyr).

Butylmethylpyridinium trifluoromethanesulfonate, [C_4mpyr][OTf]. Butylmethylpyridinium bromide (20 g, 0.087 mol) was dissolved in acetone and potassium trifluoromethanesulfonate (16.37 g, 0.087 mol) was added to the solution. The mixture was stirred for two days. Afterwards the salt was removed and the solvent was evaporated. The ionic liquid was dissolved in dichloromethane and the solvent was evaporated again. Then the product was dried in the vacuum.

^{1}H NMR (200 MHz, DMSO-d_6), δ/ppm: 1.0 (t, 3H, CH_2-CH_3), 1.4 (m, 2H, CH_2-CH_2-CH_3) 2.0 (m, 2H, CH_2-CH_2-CH_2), 2.7 (s, 3H, CH_3-pyr), 4.7 (t, 2H, N-CH_2), 8.0 (d, 2H, pyr), 9.0 (d, 2H, pyr).

Butylmethylpyridinium dicyanamide, [C_4mpyr][DCA]. Butylmethylpyridinium bromide (20 g, 0.087 mol) was dissolved in acetone and sodium dicyanamide (7.7 g, 0.087 mol) was added to the solution. The mixture was stirred for two days. Afterwards the salt was removed and the solvent was evaporated. The ionic liquid was dissolved in dichloromethane and the solvent was evaporated again. Then the product was dried in the vacuum.

^{1}H NMR (200 MHz, DMSO-d_6), δ/ppm 0.8(t, 3H, CH_2-CH_3), 1.2 (m, 2H, CH_2-CH_2-CH_3), 1.8 (m, 2H, CH_2-CH_2-CH_2), 2.6 (s, 3H, CH_3-pyr), 4.6 (t, 2H, N-CH_2), 7.9 (d, 2H, pyr), 9.0 (d, 2H, pyr).

Choline bis(trifluoromethanesulfonyl)amide, [Choline][NTf$_2$]. Choline chloride (20 g, 0.143 mol) was dissolved in water and lithium bis (trifluoromethanesulfonyl)amide (41.05 g, 0.143 mol) was added to the solution. The mixture was stirred for four hours. Next the mixture was dissolved in dichloromethane and the water layer was separated. Then the dichloromethane layer was washed with water until all halogens were removed. This was tested with a silver nitrate solution. The solvent was evaporated and the ionic liquid dried in vacuum.

^{1}H NMR (200 MHz, DMSO-d_6), δ/ppm: 3.1 (s, 9H, N-(CH_3)$_3$), 3.38 (t, 2H, CH_2-CH_2-N), 3.86 (s, 2H, OH-CH_2-CH_2), 5.16 (s, 1H, CH_2-O*H*).

Choline dicyanamide, [Choline][DCA]. Choline chloride (20 g, 0.143 mol) was dissolved in acetone and sodium dicyanamide (12.7 g, 0143 mol) was added to the solution. The mixture was stirred for two days. Afterwards the salt was removed and the solvent was evaporated. The ionic liquid was dissolved in dichloromethane and the solvent was evaporated again. Then the product was dried in the vacuum.

^{1}H NMR (200 MHz, DMSO-d_6), δ/ppm 2.8 (s, 9H, N-(CH_3)$_3$), 3.1 (t, 2H, CH_2-CH_2-N), 3.6 (m, 2H, OH-CH_2-CH_2), 5.5 (s, 1H, CH_2-O*H*).

ZnS nanoparticles. 100 mg (0.455 mmol) zinc acetate dihydrate was dissolved in 0.3 ml dimethyl sulfoxide, then 3 ml of the respective ionic liquid were added. Sodium sulfide (109.28 mg, 0.455 mmol) was added and the mixture was stirred for 15 min. Afterwards the reaction tube was inserted into the microwave and irradiated for 5 min at 60°C to ensure a homogenous solution and then for 10 min at 120°C. The product was separated by centrifugation, washed thoroughly and dried before further characterization.

CdS nanoparticles. Cadmium acetate (100 mg, 0.375 mmol) was dissolved in 0.4 ml dimethyl sulfoxide, then 3 ml ionic liquid were added. Sodium sulphide (90.12 mg, 0.375 mmol) was added and the mixture was stirred for 15 min. Afterwards the reaction tube was inserted into the microwave and irradiated for 5 min at 60°C to ensure a homogenic solution and then for 10 min at 120° C. The product was separated by centrifugation, washed thoroughly and dried before further characterization.

Results and discussion

Synthesis

ZnS and CdS nanoparticles were prepared by the reacting dimethyl sulfoxide-solutions of the respective metal acetates with sodium sulphide in various ionic liquids under microwave irradiation (5 min. at 60°C, followed by 10 min at 120°C).

The different ILs were chosen with hindsight to different abilities to interact with the solute and nanoparticles as these were found to be important in the synthesis of metal oxides (*42–44*). Due to their modular character ILs offer tuning of these properties in a unique way through the choice of the respective cation–anion combination. See Figure 1 for chemical structures and an illustration of interaction capabilities.

1-Butyl-3-methylimidazolium is to date the most frequently used cations for ILs. It contains an aromatic core which can participate in π-interactions. The aliphatic side chains can become involved in van der Waals-bonding. The ring protons, which are highly acidic and prone can act as hydrogen bond donors. In contrast, the butylmethyl pyrrolidinium cation possess neither an aromatic ring system nor acidic protons, nor sites that can get involved in hydrogen bonding. The choline cation, however, does not contain a π-system, but a –OH group which can engage in hydrogen bonding and act as a Lewis base.

Similarly, the properties of the IL anion such as the coordination power, the hydrogen acceptor/donor capacity, capability for van der Waals interaction can be varied. Dicyanamide is strongly coordinating. In contrast to this, triflate (TfO^-) and bis(trifluoromethanesulfonyl)amide (NTf_2^-) are much weaker Lewis acids, but still can act as good hydrogen bond acceptors. Tetrafluorophosphate are extremely weakly coordinating and hydrophobic (*58–61*).

XRD measurements

Powder X-ray diffraction confirms that for all ionic liquids ZnS and CdS were obtained in the cubic zinc blende form. Figure 2 shows representative XRD patterns for the samples. The recorded diffraction peaks were quite broad, as expected for nanosized crystallites. Therefore, their size has been estimated with the Scherrer equation (*61–63*).

$$= \frac{k\lambda}{\beta \cos\theta} \quad (1)$$

where D is the mean crystalline domainsize, k is a geometric factor, λ is the X-ray wavelength (λ = 709.3 nm for molybdenum), β is the FWHM (full width at half maximum) of the diffraction peak and θ is the diffraction angle. Table 1 shows the size for all synthesized nanoparticles. Depending on the IL, sizes for both materials varied between 2 and 25 nm. Certain correlations between particle size and IL characteristics can be made: When using

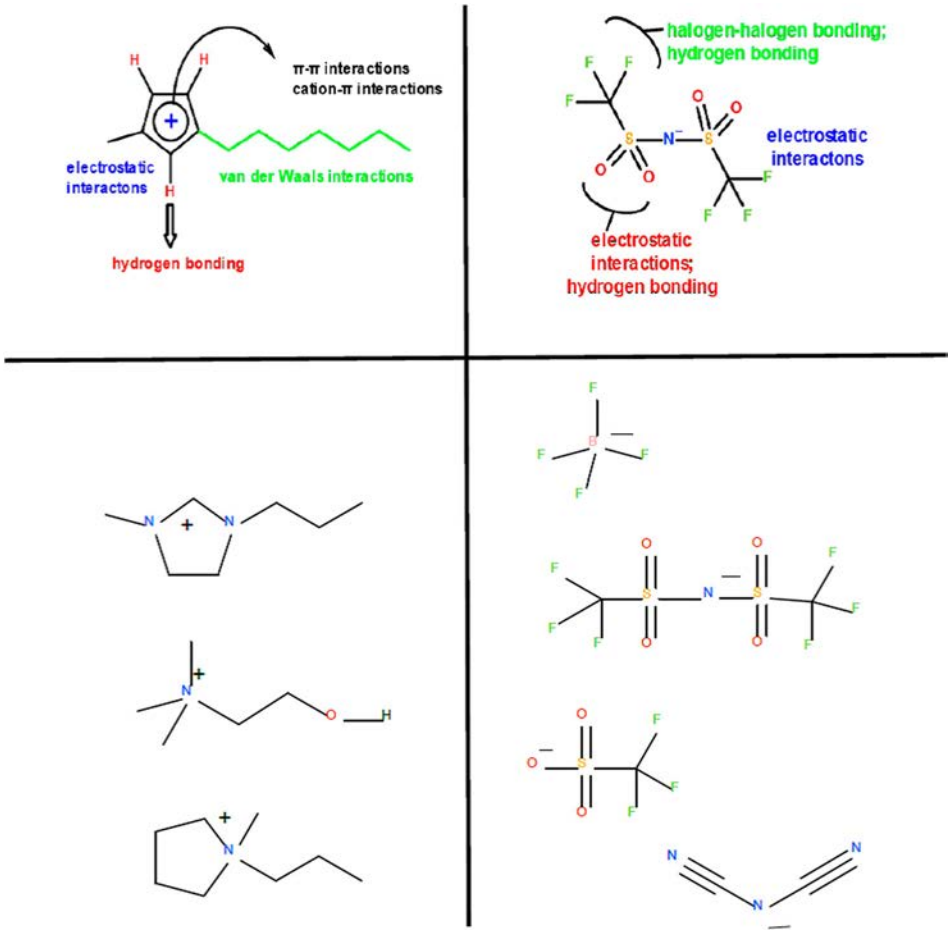

Figure 1. Ionic liquid cations (left) and anions (right) used in this study together with an illustration of potential interaction capabilities for $[C_4mim][NTf_2]$ (top).

choline as the IL cation no matter the anion, dicyanamide or bis(trifluorosulfonyl)amide, the estimated particle size was consistently small between 1.5 and 3 nm. This points to the choline cation coordinating to the particle surface and blocking any further growth. On the other hand, when using $[C_4mpyr]$-ILs the particle sizes were consistently large from 7 up to 19 nm. Here, the cation does not, aside from its positive charge, have any specific functionality that would allow for interaction with the particle surface. Particularly, when using $[C_4mim][DCA]$ large particles (24.8 nm) were obtained, both for ZnS and CdS, which shows that a coordinating anion does not have the same effect as a coordinating cations, due to its charge. It can be speculated that the ZnS and CdS surfaces are anion terminated.

Scanning electron microscopy

The real particle size may differ from the size calculated from XRD measurement, as this calculates the average size of crystalline domains, therefore does not take into account polycrystalline particles. Thus, scanning electron microscopy (SEM) was performed on selected samples to study the particle size, morphology and particle aggregation. Images confirmed the synthesis of nanoparticles (Figure 3). Exact size for the particles could not be obtained due to a maximum instrument resolution of 100 nm. However, the SEM micrographs illustrate well the particle agglomeration.

UV/Vis measurements

UV/Vis measurements were carried out using direct light reflectance mode on powder samples to determine the band gap energy for the respective semiconductor nanoparticles (see Figure 4 for representative absorption spectra). For the calculation of the band gap the wavelength of the first exciton energy was taken of each material using then the following equation,

$$E = \frac{hc}{\lambda} \tag{2}$$

where h is the Planck's constant, c is the speed of light and λ is the first exciton wavelength. The band gap

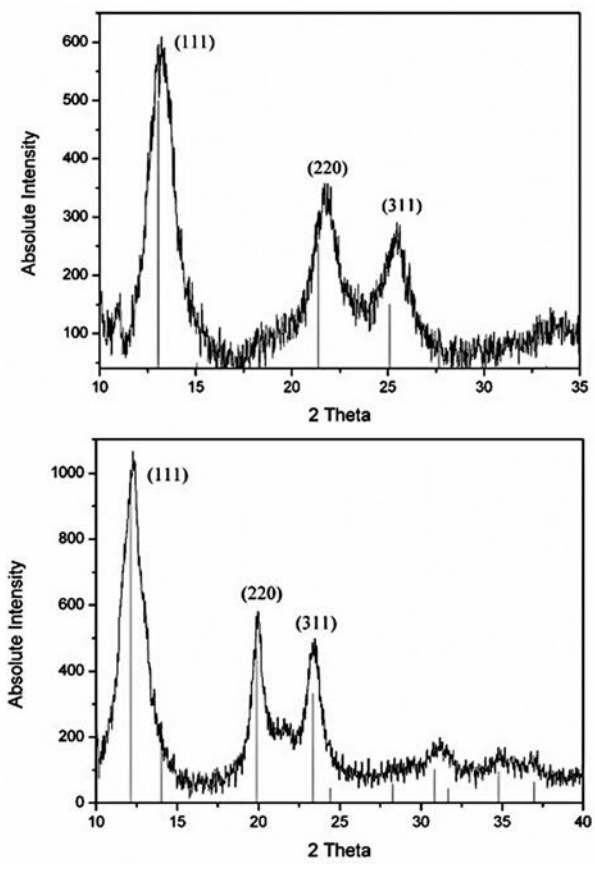

Figure 2. PXRD pattern of ZnS (top) and CdS (bottom) prepared in [Choline][NTf_2]. All diffraction peaks can be assigned to the cubic zinc blende type of structure.

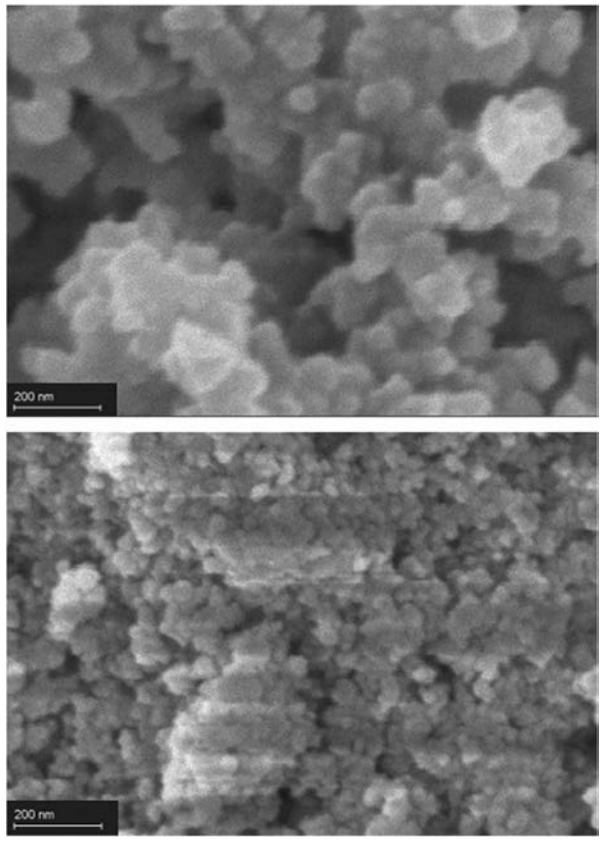

Figure 3. SEM micrographs of ZnS (top) and CdS (bottom) prepared in [Choline][NTf_2]. The scale bar is 200 nm.

energies for the prepared ZnS particles range between 3.53 and 3.91 eV, those for the prepared CdS particles between 2.47 and 3.10 eV. As expected, a relationship between the particle size and the band gap can be seen. For the prepared ZnS particles, in most cases, a band gap larger than that of the bulk is observed, which can be attributed to quantum confinement in the small particles. However, it has to be noted that an enlarged band gap is observed even well about the excitonic Bohr radius of 2.5 nm (*24*).

Table 1. Results for XRD, UV/Vis and Luminescence measurements for all samples.

Sample	Crystallite size* [nm]	Band gap [eV]	Absorption, λ_{abs}	Emission wavelength, λ_{em}
ZnS/[C_4mim][BF_4]	6.0			quenched
ZnS/[C_4mim][NTf_2]	1.5			quenched
ZnS/[C_4mim][DCA]	24.8			quenched
ZnS/[Choline][NTf_2]	2.1	3.78	345	450–500
ZnS/[Choline][DCA]	1.5	3.53	360-380; 425–500	450-525; 525–560
ZnS/[C_4mpyr][BF_4]	9.7	3.91	300-330; 580–625	500–550
ZnS/[C_4mpyr][NTf_2]	18.6	3.89	350-400; 500–550	550–600
ZnS/[C_4mpyr][OTf]	16.5	3.84	370; 475	550
ZnS/[C_4mpyr][DCA]	6.7	3.95	375; 450–500	560
CdS/[C_4mim][BF_4]	2.9	2.60		675–725
CdS/[C_4mim][NTf_2]	2.6	2.59		
CdS/[C_4mim][DCA]	24.8	3.10		700
CdS/[Choline][NTf_2]	2.9	2.58	350-400; 600 nm	600-650; 500–550
CdS/[Choline][DCA]	1.92	2.66	550–575	620–700
CdS[C_4mpyr][BF_4]	7.2	2.58		
CdS/ [C_4mpyr][NTf_2]	7.23	2.49	350-400; 550–600	650–720
CdS/[C_4mpyr][OTf]	16.5	2.47	575–625	525-575; 650–750
CdS/[C_4mpyr][DCA]	15.4	2.56	370-380; 550–600	675

*as calculated from the most intense diffraction peaks.

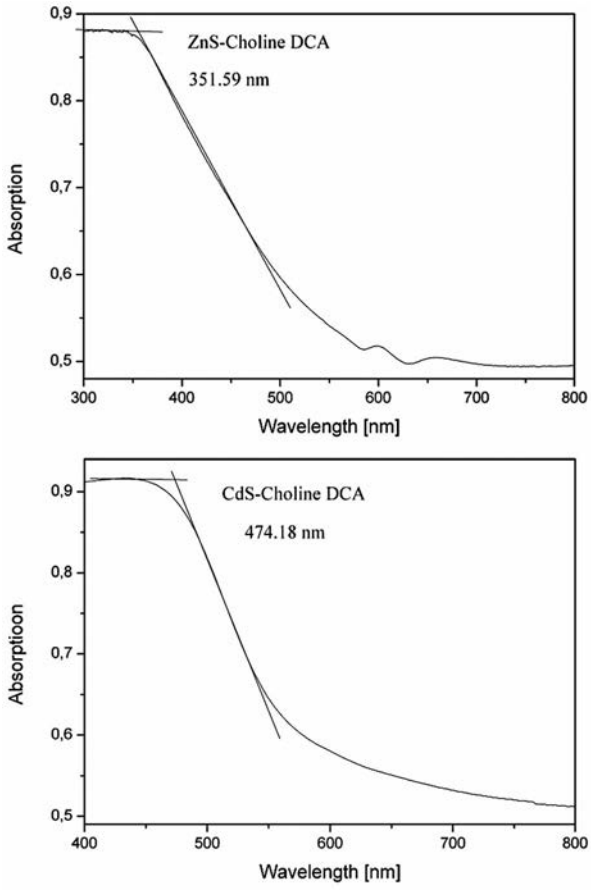

Figure 4. UV-vis absorption of ZnS (top) and CdS (bottom) prepared in [Choline][DCA].

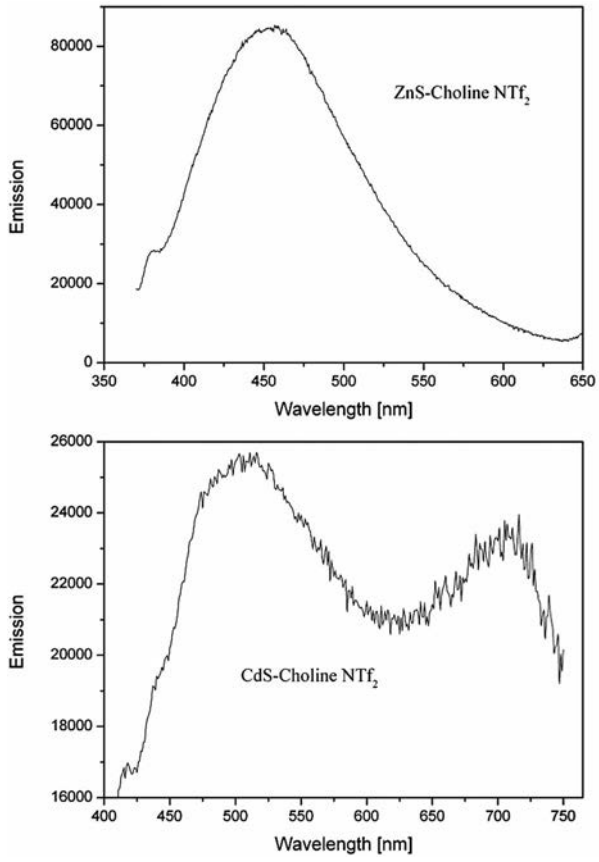

Figure 5. Photoluminescence spectrum of ZnS (top) and CdS (bottom) prepared in [Choline][NTf_2].

For CdS all samples show a band gap larger than that of the bulk (2.42 eV) (*33*). CdS prepared in [Choline][DCA] has the smallest particle (1.92 nm) and features the highest band gap energy (2.66 eV). CdS prepared in [C_4mpyr][OTf] has the larges particle size (16.5 nm) and lowest band gap (2.47 eV), albeit still larger than the bulk. Only CdS prepared in [C_4mim][DCA] is an exception with a size 24.8 nm and a band gap energy of 3.10 eV. For this particle the bulk band gap energy of CdS (2.42 eV) would be expected. This deviation could originate from impurities and defects.

Photoluminescence measurements

Photoluminescence spectra were recorded for powder samples of ZnS and CdS (see Table 1 for emission wavelength and Figure 5 for representative spectra). Interestingly, when [C_4mim]$^+$ was used as the IL-cation, the photoluminescence was completely quenched for ZnS. For the other samples, a broad emission which generally was blue shifted with respect to the bulk materials could be recorded.

Conclusions

ZnS and CdS nanoparticles were synthesized in different ILs with microwave irradiation. Powder X-ray diffraction, scanning electron microscopy and optical spectroscopy confirmed size dependent quantum confinement effects and the influence of the IL on the obtained size of both, ZnS and CdS. The syntheses are fast, energy efficient and, quite important, omit the employment of any additives to guide the NP-formation. A correlation between particle size and IL used in the reaction could be made out. Particularly, [Choline][NTf_2] led to small sulfide nanoparticles, which reveals the influence of strongly coordinating cations to block crystal growth.

Acknowledgements

The authors acknowledge institutional support from the Ruhr-Universität Bochum, Germany and Stockhoms universitet, Sweden. The Alexander-von Humboldt Foundation is acknowledged for a fellowship to P.C.; A.-V. M. acknowledges support from the Royal Swedish Academy of Science through the Göran Gustafsson prize in Chemistry as well as Energimyndigheten (grant number 46595-1).

Disclosure statement

No potential conflict of interest was reported by the author(s).

Funding

The authors acknowledge institutional support from the Ruhr-Universität Bochum, Germany and Stockhoms universitet, Sweden. The Alexander-von Humboldt Foundation is acknowledged for a fellowship to P.C.; A.-V. M. acknowledges support from the Royal Swedish Academy of Science through the Göran Gustafsson prize in Chemistry as well as Energimyndigheten (grant number 46595-1).

References

[1] Welton, T. *Green Chem.* **2011,** *13*, 225–225.
[2] Wasserscheid, P.; Keim, W. *Angew. Chem.* **2000,** *112*, 544–3945.
[3] Mudring, A.-V. *Aus. J. Chem.* **2010,** *63*, 544–564.
[4] Welton, T. *Chem. Rev.* **1999,** *99*, 2071–2083.
[5] Earle, M.J.; Seddon, K.R. *Pure Appl. Chem.* **2000,** *72*, 1–25.
[6] Antonietti, M.; Kuang, D.; Smarsly, B.; Zhou, Y. *Angew. Chem. Int. Ed.* **2004,** *43*, 4988–4992.
[7] Zhou, Y. *Curr. Nanosci.* **2005,** *1*, 35–42.
[8] Mudring, A.-V.; Alammar, T.; Bäcker, T.; Richter, K. Nanoparticle Synthesis in Ionic Liquids. In *Ionic Liquids: From Knowledge to Application*, Pechkova, N.V.; Rogers, R.D., Seddon, K.R., Eds. *ACS Symposium Series* 2009; 1030, pp. 177–188, ACS Publications, Washington D.C.
[9] Richter, K.; Campbell, P.S.; Bäcker, T.; Schimitzek, A.; Yaprak, D.; Mudring, A.-V. *Phys. Status Solidi B* **2013,** *250*, 1152–1164.
[10] Richter, K.; Birkner, A.; Mudring, A.-V. *Angew. Chem. Int. Ed.* **2010,** *49*, 2431–2435.
[11] Richter, K.; Birkner, A.; Mudring, A.-V. *Phys. Chem. Chem. Phys.* **2011,** *13*, 7136–7141.
[12] Alammar, T.; Shekhah, O.; Wohlgemuth, J.; Mudring, A.-V. *J. Mater. Chem.* **2012,** *22*, 18252–18260.
[13] Alammar, T.; Mudring, A.-V. *ChemSusChem.* **2011,** *12*, 1796–1804.
[14] Yang, M.; Campbell, P.; Santini, C.; Mudring, A.-V. *Nanoscale.* **2014,** *6*, 3367–3375.
[15] Alammar, T.; Smetana, V.; Pei, H.; Hamm, I.; Wark, M.; Mudring, A.-V. *Adv. Sus. Sys.* **2020**. https://doi.org/10.1002/adsu.202000180
[16] Lorbeer, C.; Cybinska, J.; Mudring, A.-V. *J. Mat. Chem. C* **2014,** *2*, 1862–1868.
[17] Alammar, T.; Noei, H.; Wang, Y.; Mudring, A.-V. *Nanoscale.* **2013,** *5*, 8045–8055.
[18] Heimann, S.; Schulz, S.; Schaumann, J.; Mudring, A.-V.; Stoetzel, J.; Maculewicz, F.; Schierning, G. *J. Mat. Chem. C* **2015,** *3*, 10375–10380.
[19] Schaumann, J.; Loor, M.; Ünal, D.; Mudring, A.-V.; Heimann, S.; Hagemann, U.; Schulz, S.; Maculewicz, F.; Schierning, G. *Dalton Trans.* **2017,** *46*, 656–668.
[20] Segets, D.; Lutz, C.; Yamamoto, K.; Komada, S.; Süß, S.; Mori, Y.; Peukert, W. *J. Phys. Chem. C* **2015,** *119*, 4009–4022.
[21] Thambidurai, M.; Muthukumarasamy, N.; Agilan, S.; Murugan, N.; Vasantha, S.; Balasundaraprabhu, R.; Senthil, T.S. *J. Mater. Sci.* **2010,** *45*, 3254–3258.
[22] Wells, A.F. *Structural Inorganic Chemistry* 5th ed.; Clarendon Press: Oxford, 1984.
[23] Sze, S.M.; Ng, K.K. *Physics of Semiconductor Devices*; Wiley: Hoboken, New Jersey, 2007.
[24] Gonzalez, C.M.; Wu, W.-C.; Trancy, J.B.; Martin, B. *Chem. Commun.* **2015,** *15*, 3087–3090.
[25] Ummartyotin, S.; Infahsaeng, Y. *Ren. Sus. Engery Rev.* **2016,** *55*, 17–24.
[26] Soltani, N.; Saion, E.; Hussein, M.Z.; Erfani, M.; Rezaee, K.; Bahmanrokh, G. *J. Inorg. Organomet. Polym.* **2012,** *22*, 830–836.
[27] Zhao, Y.; Hong, J.-M.; Zhu, J.-J. *J. Cryst. Growth* **2004,** *270*, 438–445.
[28] Ni, Y.; Yin, G.; Hong, J.; Xu, Z. *Mat. Res. Bull.* **2004,** *39*, 1967–1972.
[29] Borah, J.P.; Barman, J.; Sarma, K.C. *Chalcogenide Letters* **2008,** *5*, 201–208.
[30] Gayou, V.L.; Salazar-Hernández, V.L.; Delgado Macuil, R.; Zavala, G.; Santiago, P.; Oliva, A.I. *J. Nano Research* **2010,** *9*, 125–132.
[31] Pashinkin, A.S.; Kovba, L.M. *Kristallografiya* **1962,** *7*, 316–318. *Sov. Phys. Crystallogr*, 1962, *7*, 247–248.
[32] Kizilayalli, M.; Bilgin, M.; Usanmaz, A. *J. Sol. State Chem.* **1989**, *80*, 75-79.
[33] Boakye, F.; Nusenu, D. *Solid State Commun.* **1997,** *102*, 323–326.
[34] Razgoniaeva, N.; Moroz, P.; Yang, M.; Budkina, D.S.; Eckard, H.; Augspurger, M.; Khon, D.; Tarnovsky, A.N.; Zamkov, M. *J. Am. Chem. Soc.* **2017,** *139*, 7815–7822.
[35] Karan, S.; Mallik, B. *J. Phys. Chem. C* **2007,** *111*, 16734–16741.
[36] Priya, M.; Saravanan, R.S.S.; Mahadevan, C.K. *Energy Procedia* **2012,** *15*, 333–339.
[37] Tai, G.; Zhou, J.; Guo, W. *Nanotechnology* **2010,** *21*, 175601–175608.
[38] Pu, Y.; Cai, F.; Wang, D.; Wang, J.-X.; Chen, J.-F. *Ind. Eng. Chem. Res.* **2018,** *57*, 1790–1802.
[39] Evans, C.M.; Cass, L.C.; Knowles, K.E.; Tice, D.B.; Chang, R.P.H.; Weiss, E.A. *J. Coord. Chem.* **2002,** *65*, 2391–2414.
[40] Ma, M.-G.; Zhu, J.-F.; Zhu, Z.-J.; Sun, R.C. *Chem. Asian J.* **2014,** *9*, 2378–2391.
[41] Wang, Y.; Hou, Q.; Ju, M.; Li, W. *Nanomaterials* **2019,** *9*, 64. 26 pages.
[42] Alammar, T.; Slowing, I.; Anderegg, J.; Mudring, A.-V. *ChemSusChem.* **2017,** *10*, 3387–3401.
[43] Alammar, T.; Hamm, I.; Grasmik, V.; Wark, M.; Mudring, A.-V. *Inorg. Chem.* **2017,** *56*, 6920–6932.
[44] Alammar, T.; Chow, K.; Mudring, A.-V. *New J. Chem.* **2015,** *39*, 1339–1347.
[45] Lorbeer, C.; Behrends, F.; Cybinska, J.; Eckert, H.; Mudring, A.-V. *J. Mat. Chem. C* **2014,** *2*, 9439–9450.
[46] Lorbeer, C.; Cybinska, J.; Mudring, A.-V. *J. Luminescence* **2016,** *169*, 541–647.
[47] Lorbeer, C.; Mudring, A.-V. *Chem. Commun.* **2014,** *50*, 13282–13284.
[48] Lorbeer, C.; Cybinska, J.; Mudring, A.-V. *J. Mat. Chem. C* **2014,** *2*, 1862–1868.
[49] Lorbeer, C.; Mudring, A.-V. *ChemSusChem.* **2013,** *6*, 2382–2387.

[50] Campbell, P.S.; Lorbeer, C.; Cybinska, J.; Mudring, A.-V. *Adv. Funct. Mater.* **2013,** *23*, 2924–2931.
[51] Lorbeer, C.; Cybinska, J.; Mudring, A.-V. *J. Mater. Chem.* **2012,** *22*, 9505–9508.
[52] Lorbeer, C.; Cybinska, J.; Zych, E.; Mudring, A.-V. *ChemSusChem.* **2011,** *4*, 595–598.
[53] Lorbeer, C.; Cybinska, J.; Mudring, A.-V. *Chem. Commum.* **2010,** *46*, 571–573.
[54] Klauke, K.; Hahn, B.; Schütte, K.; Barthel, J.; Janiak, C. *Nano-Structures & Nano-Objects* **2015,** *1*, 24–31.
[55] Klauke, K.; Zaitsau, D.H.; Blow, M.; He, L.; Klopotowski, M.; Knedel, T.-O.; Barthel, J.; Held, C.; Verevkin, S.; Janiak, C. *Dalton Trans.* **2018**, *47*, 5083–5097.
[56] Shahid, R.; Gorlov, M.; El-Sayed, R.; Toprak, M.S.; Sugunan, A.; Kloo, L.; Muhammed, M. *Mat. Lett.* **2012,** *89*, 316–319.
[57] Esmaili, M.; Habibi-Yangheh, A. *Chin. J. Cat.* **2011,** *32*, 933–938.
[58] Devendran, P.; Alagesan, T.; Pandian, K. *Asian J. Chem.* **2013,** *25*, S79–S82.
[59] Babai, A.; Kopiec, G.; Lackmann, A.; Mallick, B.; Pitula, S.; Tang, S.-F.; Mudring, A.-V. *J. Mol. Liq.* **2014,** *92*, 191–198.
[60] Bartosik, J.; Mudring, A.-V. *Phys. Chem. Chem. Phys.* **2010,** *12*, 4005–4011.
[61] Pitula, S.; Mudring, A.-V. *Phys. Chem. Chem. Phys.* **2010,** *12*, 7056–7063.
[62] Scherrer, P. *Nachr. Ges. Wiss. Göttingen* **1918,** *26*, 98–100.
[63] Langford, J.I.; Wilson, A.J.C. *J. Appl. Cryst.* **1978,** *11*, 102–113.